Appl. Phys. B (2012) 109:593–597
DOI 10.1007/s00340-012-5179-2

Applied Physics B
Lasers and Optics

Flexible generation of optical beams with quasicrystalline structures via astigmatism induced by a tilted lens

J. C. Tung · H. C. Liang · C. H. Tsou · K. W. Su · Y. F. Chen

Received: 13 December 2011 / Revised: 8 June 2012 / Published online: 14 September 2012

Abstract We theoretically show that a family of optical beams with vortex-lattice structures can be reliably generated by tilting the focal lens to introduce the relative phases between the interfering beams. We also experimentally generate the quasicrystal beams to confirm the theoretical analysis. With the analytical wave functions and experimental patterns, a variety of vortex-lattice structures are manifested.

1 Introduction

Since the interesting demonstration of the optical Bessel beam by Durnin et al. [1], nondiffracting beams have been widely explored not only in theoretical works [2–4] but also in various applications such as minute particle trapping [5, 6], nonlinear optics [7, 8], and optical coherence tomography [9]. In fact, the nondiffracting beams cannot be exactly created due to the finite size of the focusing lens. The realizable beams with the finite energy are therefore the approximations known as the pseudo-nondiffracting beams that propagate with relatively small divergence angle. On the other hand, reliable generation of optical beams with complex crystalline and quasicrystalline structures has become increasingly important in numerous applications such as optical tweezers for multiple traps [10], spatial solitons [11], and micro-fluidic sorting [12]. It is more practically desirable and useful for emergent applications to generate optical beams simultaneously with pseudo-nondiffracting characteristics and complex lattice structures.

Multi-beam interference technique is often used to produce desired optical patterns with periodic and quasi-periodic structures [13]. Nevertheless, multi-beam interference generally requires an intricate setup to divide a laser beam into several components of equal intensity, resulting in the deficiency of stability. Recently, pseudo-nondiffracting optical beams with crystal and quasicrystal structures have been robustly generated by the Fourier-transformed method in which the desired beams are formed by using a collimated light to illuminate a mask with multiple tiny apertures regularly distributed on a ring [14–16]. The Fourier-transformed method has been also employed to create the cluster-like speckle patterns with a longer correlation beyond the speckle size [17–19]. In reality, this method generally needs a focusing lens to transform the spherical wave emanating from the mask into a plane wave. Consequently, the interference patterns are highly possible to be affected by the astigmatism that comes from the tilting angle between the central axis of the lens and the optical axis. To the best of our knowledge, the influence of this astigmatism on the beam structures has not been explored so far.

In this study, we demonstrate an experimental configuration to generate the optical quasicrystalline beams with small divergence angles. Even though the configuration is different from that reported by Durnin et al. [1], the divergence angle of the present optical beam can be reduced to be close to that of the conventional pseudo-nondiffracting beam. We also analyze the influence of the tilting angle α between the central axis of the lens and the optical axis on the formation of optical beams. We find that the tilting angle α can introduce a special kind of relative phases between the interfering beams. Numerical calculations reveal that the

J. C. Tung · H. C. Liang · C. H. Tsou · K. W. Su · Y. F. Chen (✉)
Department of Electrophysics, National Chiao Tung University, 1001 TA Hsueh Road, 30010 Hsinchu, Taiwan
e-mail: yfchen@cc.nctu.edu.tw

tilting angle α can turn into a beneficial parameter to generate quasicrystal beams more flexibly. We further experimentally generate a variety of quasicrystal beams to confirm the numerical results of theoretical analysis. Finally, we employ the derived wave function to analyze the experimental beams to manifest the structures of vortex lattices.

2 Theoretical analysis

For an ideal thin lens normal to the optical axis in the z direction, the phase delay suffered by the wave at coordinates (ξ, η) is given by

$$\phi(\xi,\eta) = \phi_o - \frac{k}{2f}\left(\xi^2 + \eta^2\right), \tag{1}$$

where ϕ_o is the delay at the center, f is the focal length, $k = 2\pi/\lambda$, and λ is the wavelength of the coherent light. When the thin lens has a tilting angle α with respect to the x-axis at $z = 0$, the coordinates of the lens can be denoted as (x', y'), where $x' = \xi\cos\alpha$ and $y' = \eta$. Thus, the phase factor may be expressed as

$$\phi(x',y') = \phi_o - \frac{k}{2f}\left(x'^2/\cos^2\alpha + y'^2\right) \tag{2}$$

Ignoring the constant phase and using the Fresnel diffraction theory, the complex amplitude $u(x, y, z)$ of the field behind the lens with a tilting angle α for the input complex amplitude $u_o(x, y)$ of the field just in front of the lens can be derived to be

$$u(x,y,z) = \frac{-i}{\lambda z}\, e^{ik\left(z+\frac{x^2+y^2}{2z}\right)} \iint u_o(x',y')\, e^{-i\frac{k}{2f}(x'^2\tan^2\alpha)}\, e^{-i\frac{k}{2f}\left(1-\frac{f}{z}\right)(x'^2+y'^2)} \times e^{-i\frac{k}{z}(xx'+yy')}\, dx'\, dy' \tag{3}$$

Now consider a mask with multiple apertures (small circular holes) regularly distributed on a ring to be illuminated with collimated light. In terms of polar coordinates (ρ', ϕ'), the field just after the mask can be approximately expressed as

$$u_o(\rho',\ \varphi') = (1/q)\frac{\delta(\rho'-a)}{\rho'}\sum_{s=0}^{q-1}\delta\left(\varphi' - \frac{2\pi s}{q}\right), \tag{4}$$

where a is the radius of the ring, q is a positive integer, and $\delta(\bullet)$ is the Dirac delta function. Substituting Eq. (4) into Eq. (3) and performing the integration, the output field can be found to be

$$u(\rho,\phi,z) = \frac{-i\,a}{\lambda z}\, e^{ik\left(z+\frac{\rho^2}{2z}\right)}\, e^{-i\frac{k\rho^2}{2f}\left(1-\frac{f}{z}\right)}\Psi_q(\rho,\phi,z;\alpha) \tag{5}$$

and

$$\Psi_q(\rho,\phi,z;\alpha) = (1/q)\sum_{s=0}^{q-1} e^{-i\frac{k a^2\tan^2\alpha}{2f}\left(\cos\frac{2\pi s}{q}\right)^2}\, e^{-i\frac{k a}{z}\rho\cos\left(\phi-\frac{2\pi s}{q}\right)}. \tag{6}$$

We can find that the output field represents a quasicrystalline beam formed by q plane waves with the specific relative phases related to the tilting angle α. Note

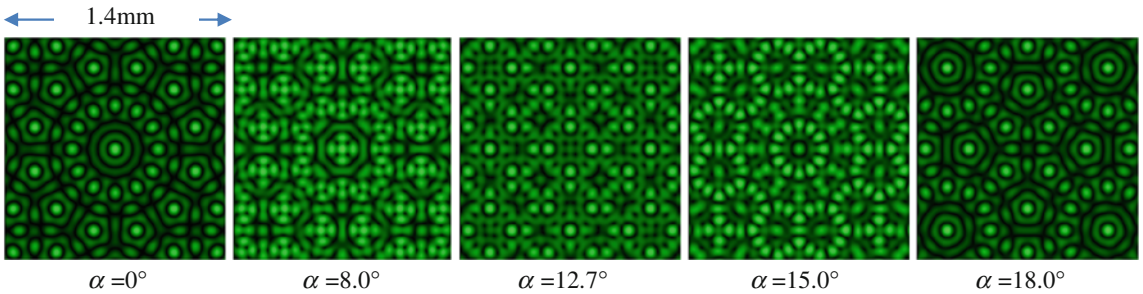

Fig. 1 Numerical patterns for the intensity $\left|\Psi_q(\rho,\phi,z;\alpha)\right|^2$ with various tilting angles α for the case of $q = 12$, $a = 5$ mm, $z = f = 1{,}000$ mm, and $\lambda = 632.8$ nm

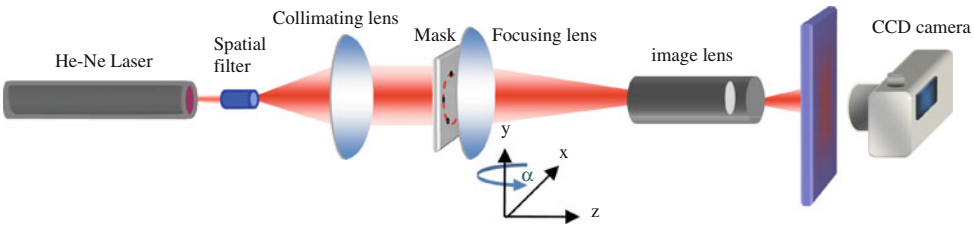

Fig. 2 Experimental setup for realizing the pseudo-nondiffracting beams with the vortex-lattice structures

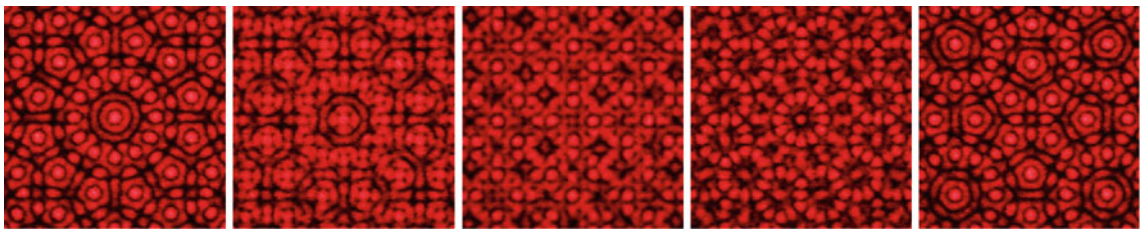

Fig. 3 Experimental interference patterns for $q = 12$ quasicrystal structures corresponding to the numerical cases shown in Fig. 1

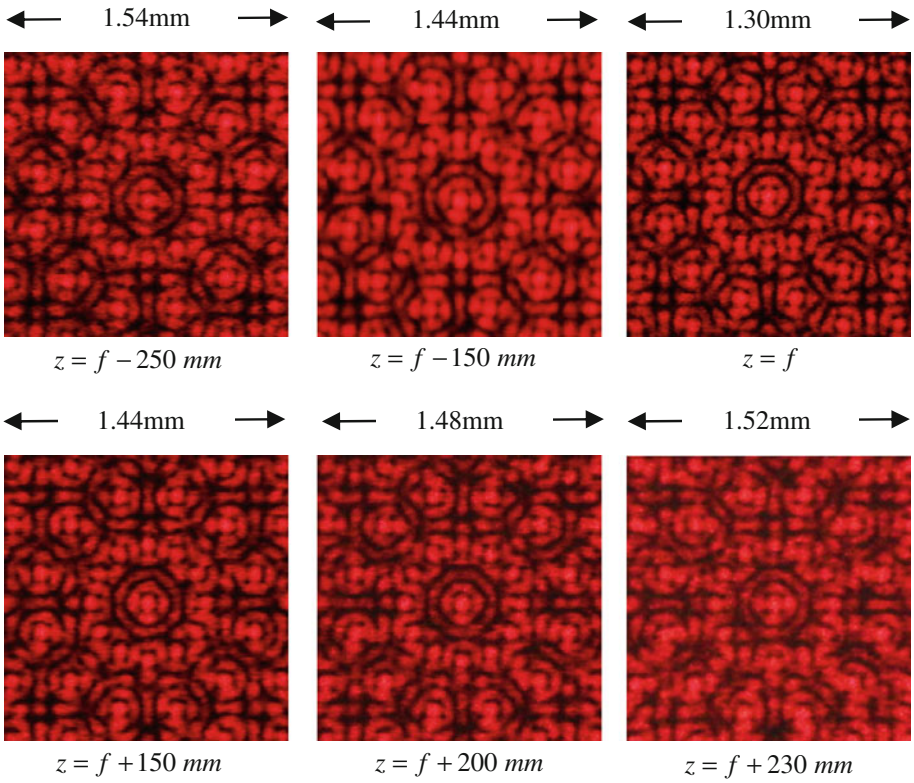

Fig. 4 Experimental generated quasicrystal patterns by rotating the focusing lens to the angle $\alpha = 8.0°$ for $q = 12$ at different propagation distances along z

that Eq. (6) is derived with an infinitesimal pinhole. For a genuine small pinhole, the quasicrystalline pattern can be really generated at the position after the focusing lens with $z > 0.5\,f$. Furthermore, the divergent angle of the optical beam in Eq. (6) can be derived to be $\theta \approx \sin\theta = a/f$. In the Durnin's approach [1], the divergence angle of the generated beam is given by $\theta = a^2/Rf$ because of the finite geometric radius R of the focusing lens. From a practical point of view, the present optical beam with the help of lowering the ratio a/f can have the divergence angle to be as small as that of the pseudo-nondiffracting beam generated with the Durnin's approach. If $\alpha = 0$, the wave function $\psi_q(\rho,\phi,z;\alpha)$ turns out to be the standard representations for the crystal and quasicrystal waves with all interfering beams in phase. For $q \to \infty$, the wave function $\Psi_q(\rho,\phi,z;\alpha)$ approaches to the form of the zero-order Bessel beam: $\Psi_{q\to\infty}(\rho,\phi,z;\alpha) = (1/2\pi)\,J_0(ka\rho/z)$.

Figure 1 depicts the calculated patterns for the intensity $\left|\Psi_q(\rho,\phi,z;\alpha)\right|^2$ with various angles α for the case of $q = 12$, $a = 5$ mm, $z = f = 1{,}000$ mm, and $\lambda = 632.8$ nm. It can be seen that a variety of rich quasi-crystal wave patterns can be constructed by controlling the tilting angle α. This result indicates that the tilting angle α can turn into a beneficial parameter to generate quasicrystal beams more flexibly. In the following, we perform an experiment to confirm the numerical results of theoretical analysis.

3 Experimental setup and results

Figure 2 depicts the experimental setup for realizing the beams with the crystalline and quasicrystalline structures described in Eq. (5). As a parallel light beam is formed by

using the collimating lens, the mask was placed just in front of the focusing lens with the focal length of 1,000 mm. Moreover, the mask closing to the focusing lens could simplify the numerical calculations. The light source was a linearly polarized 20-mW He–Ne laser with a wavelength of 632.8 nm. Light from the He–Ne laser was focused to a point at a pinhole by a lens of short focal length, where the lens/pinhole arrangement was used as a spatial filter. A collimating lens, of focal length 100 mm, was placed at a distance 100 mm from the plane of the pinhole to collimate the laser light with the divergence angle <0.1 mrad. We employed a laser stencil-cutting machine to precisely fabricate the metal masks with tiny circular holes regularly distributed on a ring, where the radii of the hole and the ring were 0.1–5.0 mm, respectively. The focusing lens was mounted on a rotational stage for tailoring the tilting angle with respect to the x-axis. Interference patterns formed in the back focal plane were imaged with a microscope lens and a CCD camera.

Figure 3 depicts the experimental interference patterns for $q = 12$ quasicrystal structures observed by rotating the focusing lens to the different angles corresponding to the numerical cases shown in Fig. 1. It can be seen that the experimental observations agree very well with the numerical patterns shown in Fig. 1. Figure 4 shows the experimental-generated quasicrystal patterns by rotating the focusing lens to the angle $\alpha = 8.0°$ for $q = 12$ at different propagation distances along z. The patterns can be clearly seen to be diffraction free over a finite distance which called propagation-invariant region. The excellent agreement validates the theoretical analysis and confirms the experimental approach. Figure 5 shows the experimental and numerical quasicrystal patterns for the case of $q = 30$. Once again, the experimental results are in good agreement with the numerical calculations. More intriguingly, the beams $\Psi_q(\rho, \phi, z; \alpha)$ for the high order case exhibit exotic kaleidoscopic wave patterns.

As the relative phases between the interfering beams are explicitly introduced by tilting the focal lens, the resultant

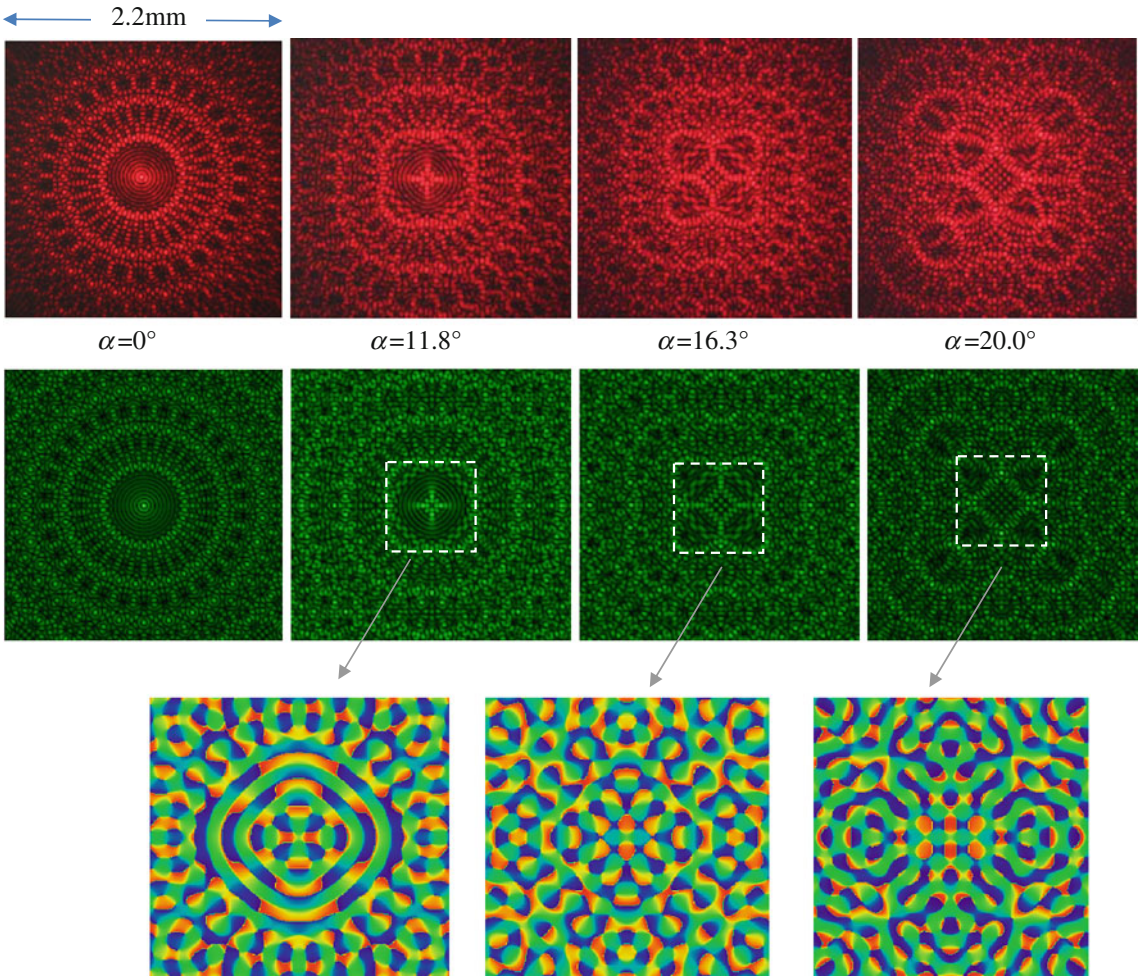

Fig. 5 Experimental (the *first row*) and numerical (the *second row*) quasicrystal patterns for the case of $q = 30$. In the *last row* contour plots of phase fields $\Theta(\rho, \phi)$ for the *boxed* regions shown in the *second row*

beams generally belong to a field containing phase singularities, such as vortices. Phase singularities of the complex fields are characterized by isolated dark spots, where phases are ambiguous and amplitudes are zero. Light beams possessing phase singularities, or optical vortices [20, 21] have been extensively explored in modern optics over the last two decades because they can be exploited in a variety of applications which includes trapping and rotation of micron and submicron objects in hydrodynamics and biology, phase contrast microscopy, and spiral interferometry. Phase singularities can be manifested with the phase angle field $\Theta(\rho, \phi) = \arctan(\mathrm{Im}[\Psi_q(\rho, \phi, z; \alpha)]/\mathrm{Re}[\Psi_q(\rho, \phi, z; \alpha)])$, where $\mathrm{Re}[\Psi_q(\rho, \phi, z; \alpha)]$ and $\mathrm{Im}[\Psi_q(\rho, \phi, z; \alpha)]$ are the real and imaginary parts of the field $\Psi_q(\rho, \phi, z; \alpha)$. The phase angle $\Theta(\rho, \phi)$ of the field $\Psi_q(\rho, \phi, z; \alpha)$ is undefined in all the vortex singularities. The last row of Fig. 5 depicts the contour plots of phase fields $\Theta(\rho, \phi)$ for the boxed regions shown in the second row of Fig. 5. The features of phase singularities in the field $\Psi_q(\rho, \phi, z; \alpha)$ can be clearly seen to display various vortex-lattice structures.

4 Conclusion

We have theoretically demonstrated a simple way to generate the quasicrystalline beams. It has been verified that tilting the focal lens can cleverly introduce a variety of relative phases between the interfering beams to generate the quasicrystal beams with vortex lattices. We also employed the derived wave function to numerically manifest the dependence of quasicrystal wave patterns on the tilting angle. Furthermore, we set up an experiment for generating beams with various quasicrystal wave patterns by means of tilting the focal lens. The excellent agreement between the numerical and experimental wave patterns confirmed the theoretical analysis. Finally, the analytical wave function was used to manifest the quasicrystal vortex lattices for the experimental beams.

Acknowledgments The authors thank the National Science Council for their financial support of this research under Contract No. NSC-100-2628-M-009-001-MY3.

References

1. J. Durnin, J.J. Miceli, J.H. Eberly, Phys. Rev. Lett. **58**, 1499–1502 (1987)
2. J. Durnin, J. Opt. Soc. Am. A **4**, 651–654 (1987)
3. G. Indebetouw, J. Opt. Soc. Am. A **6**, 150–152 (1989)
4. Z. Bouchal, Czech J. Phys. **53**, 537–578 (2003)
5. K. Dholakia, P. Reece, M. Gu, Chem. Soc. Rev. **37**, 42–55 (2007)
6. K. Volke-Sepúlveda, R. Jáuregui, J. Phys. At. Mol. Opt. Phys. **42**, 085303 (2009)
7. P. Xie, Z.Q. Zhang, Phys. Rev. Lett. **91**, 213904 (2003)
8. H. Martin, E.D. Eugenieva, Z. Chen, D.N. Christodoulides, Phys. Rev. Lett. **92**, 123902 (2004)
9. Z. Ding, H. Ren, Y. Zhao, J.S. Nelson, Z. Chen, Opt. Lett. **27**, 243–245 (2002)
10. M.M. Burns, J.M. Fournier, J.A. Golovchenko, Science **249**, 749–754 (1990)
11. N. Efremidis, S. Sears, D. Christodoulides, J. Fleischer, M. Segev, Phys. Rev. E **66**, 46602 (2002)
12. J.M. Macdonald, G. Spalding, K. Dholakia, Nature **426**, 421–424 (2003)
13. X. Wang, C.Y. Ng, W.Y. Tam, C.T. Chan, P. Sheng, Adv. Mater. **15**, 1526 (2003)
14. Y.F. Chen, H.C. Liang, Y.C. Lin, Y.S. Tzeng, K.W. Su, K.F. Huang, Phys. Rev. A **83**, 053813 (2011)
15. J. Xavier, M. Boguslawski, P. Rose, J. Joseph, C. Denz, Adv. Mater. **22**, 356–360 (2010)
16. V. Arrizón, D. Sánchez-de-la-Llave, G. Méndez, U. Ruiz, Opt. Express **23**, 10553–10562 (2011)
17. K. Uno, J. Uozumi, T. Asakura, Opt. Commun. **114**, 203–210 (1995)
18. A. Lencina, M. Tebaldi, P. Vaveliuk, N. Bolognini, Waves Random Complex Media **17**, 29–42 (2007)
19. E. Mosso, M. Tebaldi, A. Lencina, N. Bolognini, Opt. Commun. **283**, 1285–1290 (2010)
20. J.F. Nye, M.V. Berry, Proc. R Soc. London Ser. A **336**, 165 (1974)
21. M.S. Soskin and M.V. Vasnetsov, Singular optics, ed. by E. Wolf, *Progress in Optics*, vol 42 (Elsevier, Amsterdam, 2001), p. 219